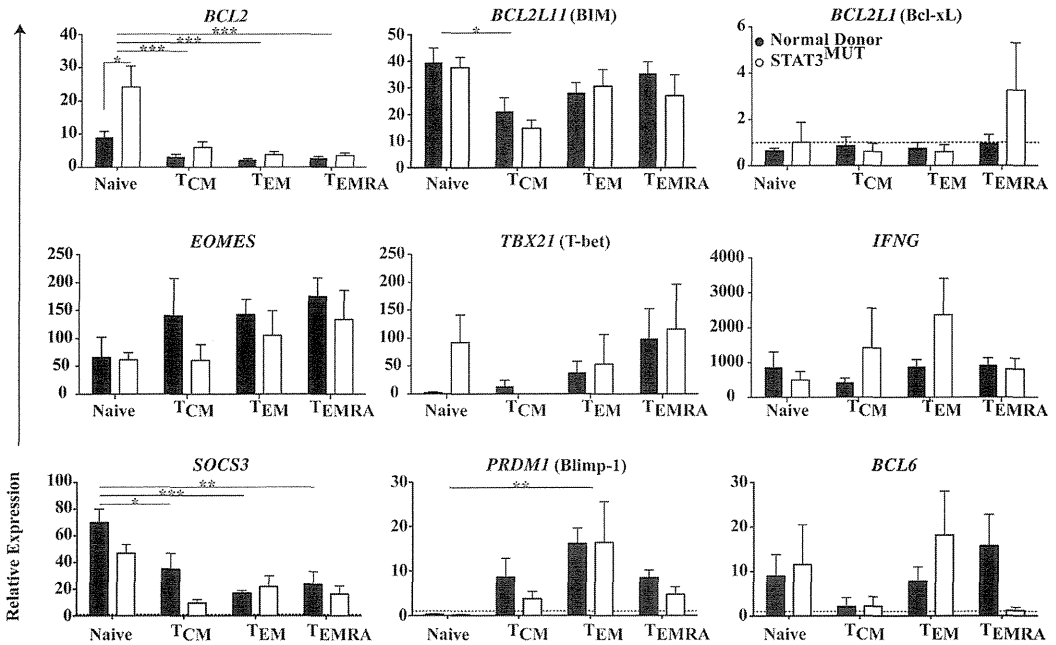

FIG E1. Differential expression of transcription factors and apoptotic family members in subsets of $CD8^+$ T cells. Expression of the proapoptotic regulator *BCL2* and the antiapoptotic regulators *BCL2L11* and *BCL2L1*; the transcription factors *EOMES*, *TBX21*, *SOCS3*, *PRDM1*, and *BCL6*; and the cytokine *IFNG* was determined in sorted purified subsets of $CD8^+$ T cells from normal donors and STAT3-deficient patients by means of quantitative PCR. The results are means ± SEMs (n = 5) and are expressed relative to glyceraldehyde-3-phosphate dehydrogenase *(GAPDH)*. $^*P < .05$, $^{**}P < .01$, and $^{***}P < .001$.

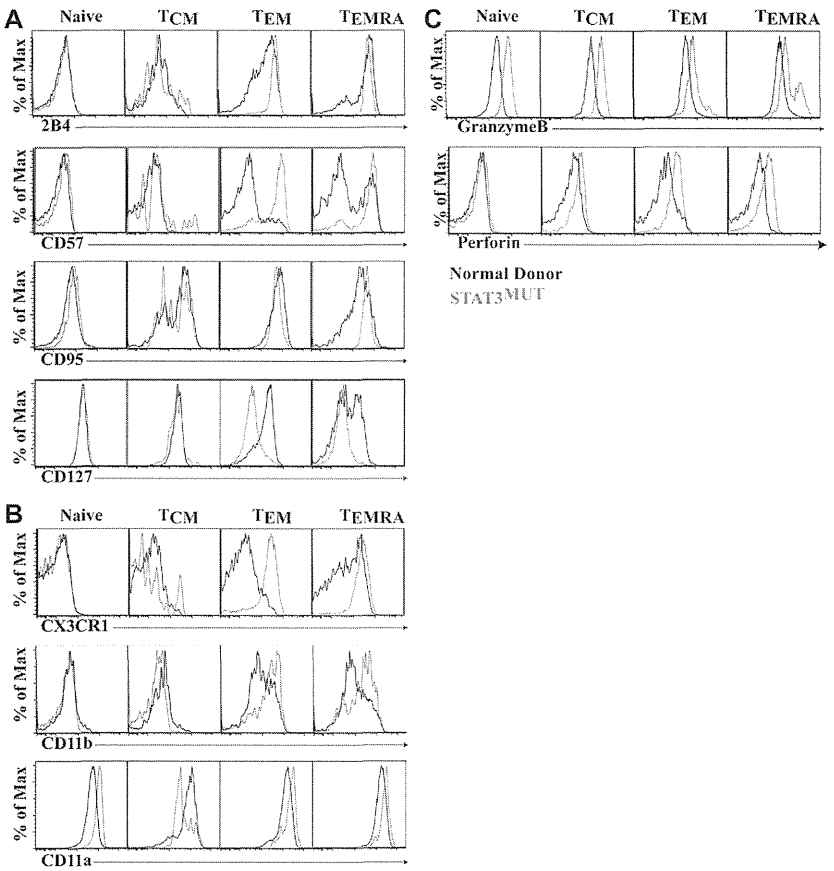

FIG E2. The *ex vivo* phenotype of STAT3-deficient $CD8^+$ T cells. **A-C,** Naive, T_{CM}, T_{EM}, and T_{EMRA} $CD8^+$ T cells in PB of normal donors *(black histogram)* and STAT3-deficient patients *(gray histogram)* were assessed for expression of 2B4, CD57, CD95, CD127, CX3CR1, CD11a, CD11b, granzyme B, or perforin. Histogram plots are from 1 representative healthy donor and 1 STAT3-deficient patient.

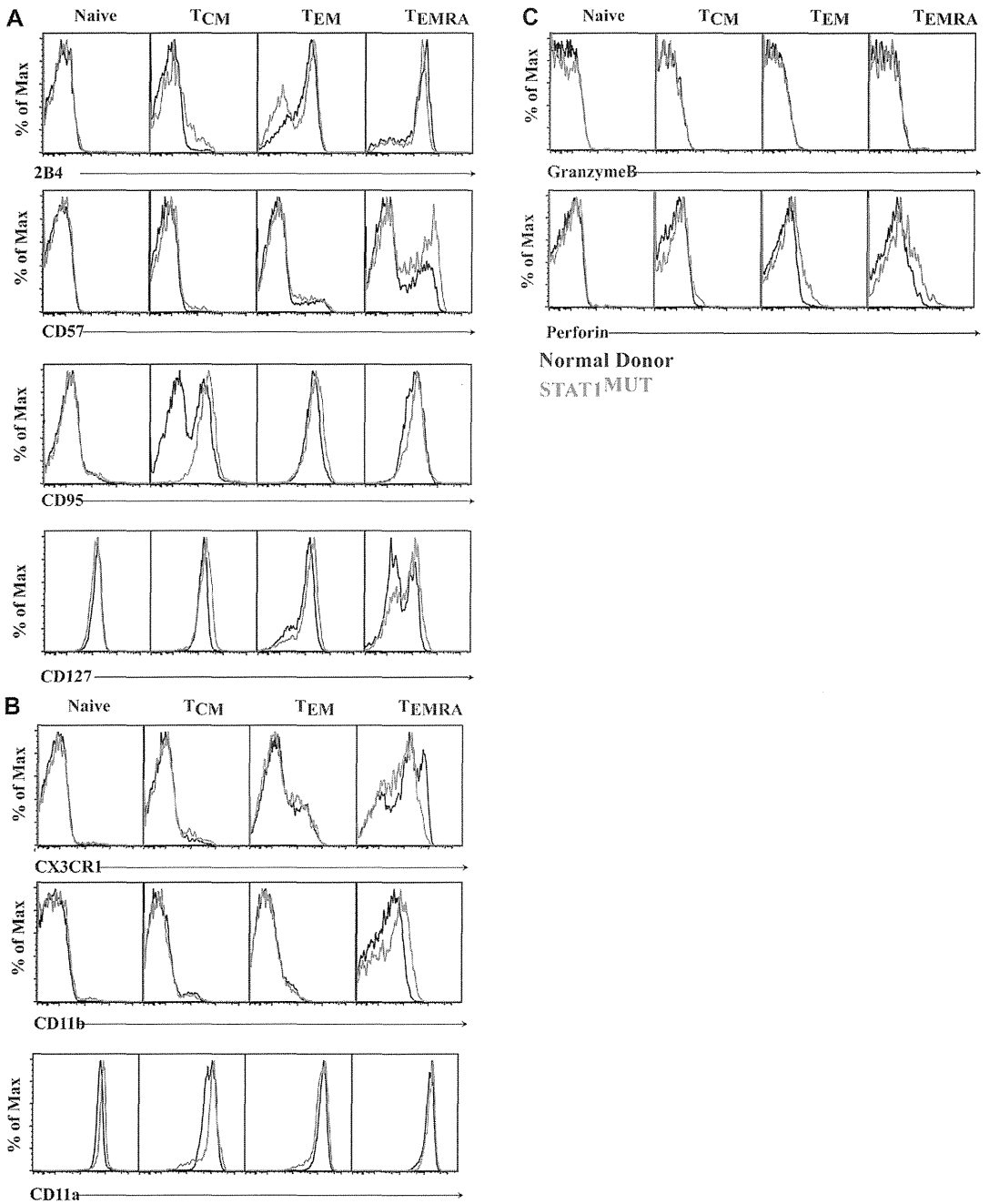

FIG E3. The *ex vivo* phenotype of STAT1-deficient $CD8^+$ T cells. **A-C,** Naive, T_{CM}, T_{EM}, and T_{EMRA} $CD8^+$ T cells in PB of normal donors *(black histogram)* and STAT1-deficient patients *(gray histogram)* were assessed for expression of 2B4, CD57, CD95, CD127, CX3CR1, CD11a, CD11b, granzyme B, or perforin. Histogram plots are from 1 representative healthy donor and 1 STAT1-deficient patient.

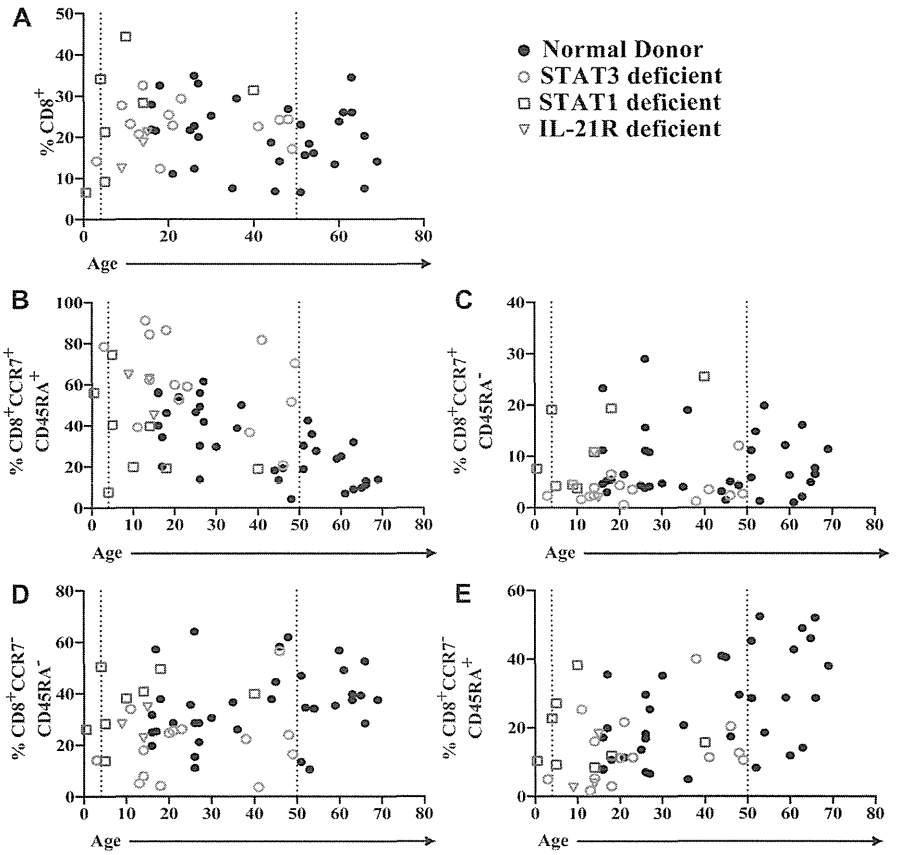

FIG E4. $CD8^+$ T-cell subsets in STAT3-deficient and STAT1-deficient patients. **A-E,** Percentages of $CD8^+$ (Fig E4, *A*), naive (Fig E4, *B*), T_{CM} (Fig E4, *C*), T_{EM} (Fig E4, *D*), and T_{EMRA} (Fig E4, *E*) cells are plotted against the age of each subject at the time the PB samples were analyzed from healthy donors (n = 31), STAT3-deficient patients (n = 14), STAT1-deficient patients (n = 8), or IL-21R–deficient patients (n = 3). Each value represents an individual donor or patient.

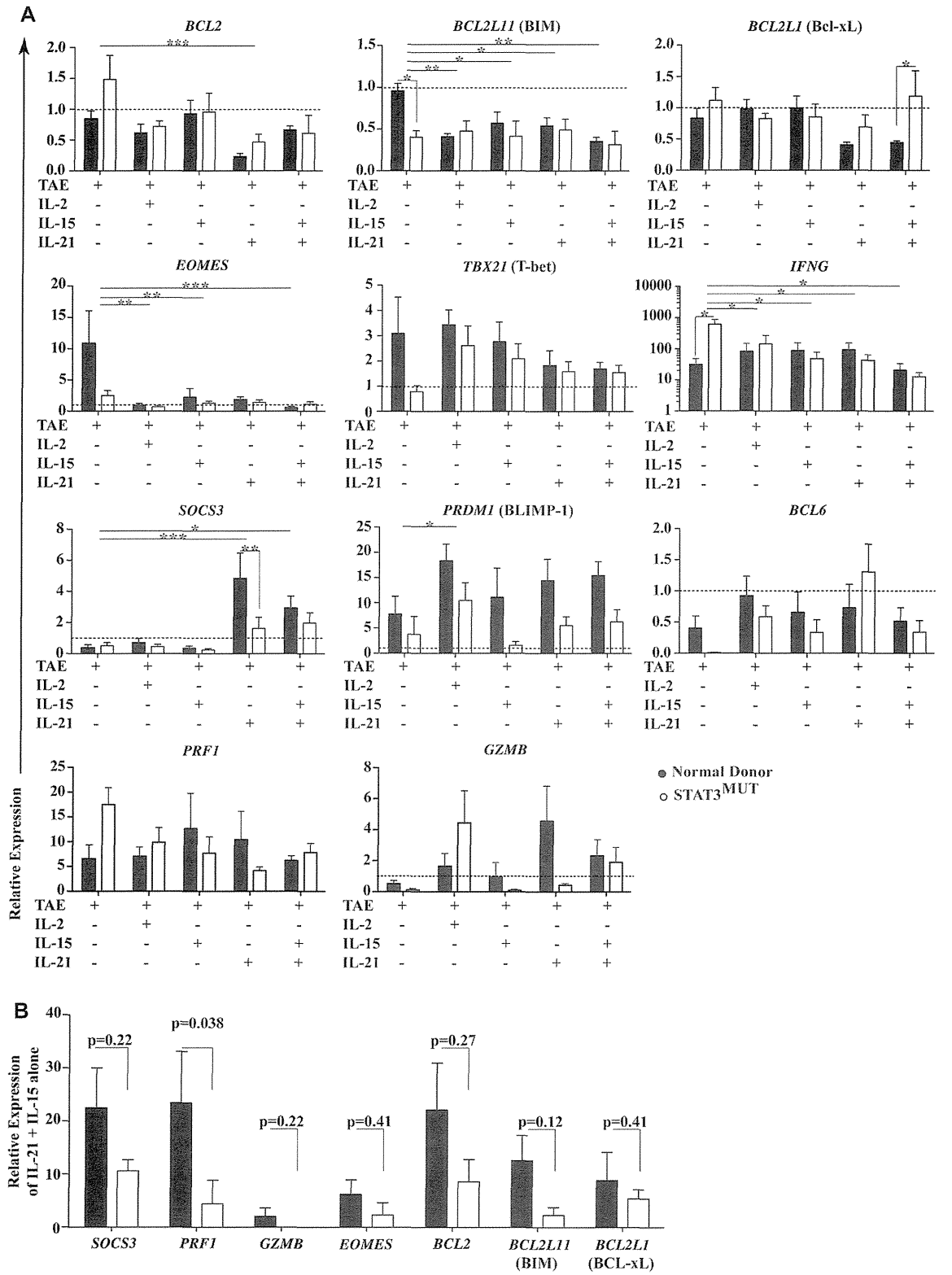

FIG E5. Differential expression of transcription factors and apoptotic family members in cultured naive $CD8^+$ T cells. Expression of the proapoptotic regulator *BCL2* and the antiapoptotic regulators *BCL2L11* and *BCL2L1*; the transcription factors *EOMES*, *TBX21*, *SOCS3*, *PRDM1*, and *BCL6*; and the effector molecules *IFNG*, *GZMB*, and *PFR1* was determined by means of quantitative PCR in naive $CD8^+$ T cells from normal donors and STAT3-deficient patients that were cultured for either 4 days with TAE beads in the absence or presence of the indicated cytokines **(A)** or for 10 days with IL-21 and IL-15 alone **(B)**. The results are means ± SEMs (n = 4-7) and expressed relative to glyceraldehyde-3-phosphate dehydrogenase *(GAPDH)*. $*P < .05$, $**P < .01$, and $***P < .001$.

TABLE E1. Patients with PIDs

Disease	Patient ID	Mutation/genotype	Age at analysis (y)	References
AD-HIES	HIES#1	R382Q	20	E1-E4
(STAT3 deficiency)	HIES#2	V637M	21	
(Heterozygous)	HIES#4	H437P	11	
	HIES#5	Q644P	46	
	HIES#6	S465F	13	
	HIES#7	Y657N	48	
	HIES#8	R382W	9	
	HIES#9+	L706M	23	
	HIES#10+	L706M	49	
	HIES#11	R382W	14	
	HIES#13*	V463Δ	18	
	HIES#14*	V463Δ	41	
	HIES#15	R539P	14	
	HIES#16	V463Δ	38	
	HIES#17	F621L	3	
MSMD + viral infection	$STAT1_{MUT}1$	1928insA (homozygous)	0.5	E5,E6
(STAT1 deficiency)	$STAT1_{MUT}2$†	P696S (homozygous)	18	
	$STAT1_{MUT}3$†	P696S (homozygous)	14	
MSMD only	$STAT1_{MUT}4$	Q463H/WT	10	E7,E8
	$STAT1_{MUT}5$	L706S/WT	5	
(STAT1 deficiency)	$STAT1_{MUT}9$	E320Q/WT	4	
	$STAT1_{MUT}10$‡	Y701C/WT	40	E9
	$STAT1_{MUT}11$‡	Y701C/WT	5	
IL-21R deficiency	$IL21R_{MUT}1$§	C81_H82del (homozygous)	9	E10
	$IL21R_{MUT}2$§	C81_H82del (homozygous)	14	E10
	$IL21R_{MUT}3$	W138S (homozygous)	15.5	Unpublished

MSMD, Mendelian susceptibility to mycobacterial disease.
+,*,†,‡,§Related subjects.

TABLE E2. Primary mAbs

mAb	Clone	Company
CCR7-FITC	150503	R&D Systems, Minneapolis, Minn
Phospho-STAT5–A488		BD, Franklin Lakes, NJ
CD11b-PE	D12	BD
CD45RO-PE	UCHL1	eBioscience, San Diego, Calif
CD57-PE	HCD57	BioLegend, San Diego, Calif
CD95-PE	DX2	BD
244-PE	2B4; C1.7	Beckman Coulter, Fullerton, Calif
Perforin-PE	dG9	eBioscience
Phospho-STAT3–PE		BD
CD45RA-PerCpCy5.5	HI100	eBioscience
CD8-PeCy7	RPA-T8	BD
CD28-PeCy7	CD28.2	BioLegend
CD11a-APC	HI111	BD
CD27-APC	O323	eBioscience
CX3CR1-APC	2A9-1	BioLegend
Granzyme B–APC	GB11	Invitrogen, Carlsbad, Calif
Phospho-STAT1–A647		BD
CD27-APC.Cy7	O323	BioLegend
CD8-Pacific Blue	RPA-T8	BD
CD4-e450	OKT-4	eBioscience
CD127-e450	eBioRDR5	eBioscience

APC, Allophycocyanin; *FITC*, fluorescein isothiocyanate; *PE*, phycoerythrin; *PerCP*, peridinin-chlorophyll-protein complex.

TABLE E3. Real-time PCR primers

Gene	Forward	Reverse
BCL2	5′-ttgacagaggatcatgctgtactt-3′	5′-atctttatttcatgaggcacgtt-3′
BCL2L11/BIM	5′-catcgcggtattcggttc-3′	5′-gctttgccatttggtctttttt-3′
BCL2L1/Bcl-xL	5′-tttctccttcggcggggcact-3′	5′-aaaagtatcccagccgccgttc-3′
BCL6	5′-gagctctgttgattcttagaactgg-3′	5′-gccttgcttcacagtccaa-3′
EOMES	5′-gtggggaggtcgaggttc-3′	5′-tgttctggaggtccatggtag-3′
GAPDH	5′-ctctgctcctcctgttcgac-3′	5′-acgaccaaatccgttgactc-3′
GZMB	5′-agatgcaaccaatcctgctt-3′	5′-catgtcccccgatgatct-3′
IFNG	5′-ggcattttgaagaattggaaag-3′	5′-tttggatgctctggtcatctt-3′
PRDM1/BLIMP-1	5′-aacgtgtgggtacgaccttg-3′	5′-attttcatggtccccttggt-3′
PRF1	5′-ccgcttctctatacgggattc-3′	5′-gcagcagcaggagaaggat-3′
SOCS3	5′-agacttcgattcgggacca-3′	5′-aacttgctgtgggtgacca-3′
TBX21/T-BET	5′-tgtggtccaagtttaatcagca-3′	5′-tgacaggaatgggaacatcc-3′

Heterozygosity for the Y701C *STAT1* mutation in a multiplex kindred with multifocal osteomyelitis

Osamu Hirata,[1] Satoshi Okada,[1,2] Miyuki Tsumura,[1] Reiko Kagawa,[1] Mizuka Miki,[1] Hiroshi Kawaguchi,[1] Kazuhiro Nakamura,[1] Stéphanie Boisson-Dupuis,[2,3] Jean-Laurent Casanova,[2,3] Yoshihiro Takihara,[4] and Masao Kobayashi[1]

[1]Department of Pediatrics, Hiroshima University Graduate School of Biomedical & Health Sciences, Hiroshima, Japan; [2]St. Giles Laboratory of Human Genetics of Infectious Diseases, Rockefeller Branch, The Rockefeller University, New York, NY, USA; [3]Laboratory of Human Genetics of Infectious Diseases, Necker Branch, Inserm U980 and University Paris Descartes, Necker Medical School, Paris, France, EU; [4]Department of Stem Cell Biology, Research Institute for Radiation Biology and Medicine, Hiroshima University, Hiroshima, Japan

ABSTRACT

Heterozygosity for dominant-negative *STAT1* mutations underlies autosomal dominant Mendelian susceptibility to mycobacterial diseases. Mutations conferring Mendelian susceptibility to mycobacterial diseases have been identified in the regions of the *STAT1* gene encoding the tail segment, DNA-binding domain and SH2 domain. We describe here a new heterozygous mutation, Y701C, in a Japanese two-generation multiplex kindred with autosomal dominant Mendelian susceptibility to mycobacterial diseases. This mutation affects precisely the canonical STAT1 tyrosine phosphorylation site. The Y701C STAT1 protein is produced normally, but its phosphorylation is abolished, resulting in a loss-of-function for STAT1-dependent cellular responses to interferon-γ or interferon-α. In the patients' cells, the allele is dominant-negative for γ-activated factor-mediated responses to interferon-γ, but not for interferon-stimulated gene factor-3-mediated responses to interferon-α/β, accounting for the clinical phenotype of Mendelian susceptibility to mycobacterial diseases without severe viral diseases. Interestingly, both patients displayed multifocal osteomyelitis, which is often seen in patients with Mendelian susceptibility to mycobacterial diseases with autosomal dominant partial IFN-γR1 deficiency. Multifocal osteomyelitis should thus prompt investigations of both STAT1 and IFN-γR1. This experiment of nature also confirms the essential role of tyrosine 701 in human STAT1 activity *in natura*.

Introduction

Mendelian susceptibility to mycobacterial diseases (MSMD) (OMIM 209950) is a rare congenital disorder characterized by susceptibility to clinical diseases caused by weakly virulent mycobacteria, such as *Mycobacterium bovis* Bacille Calmette-Guérin (BCG) and non-tuberculous mycobacteria.[1,2] Affected individuals are also susceptible to *M. tuberculosis*, a more virulent mycobacterial species.[3] Nine MSMD-causing genes (*IFNGR1, IFNGR2, IL12B, IL12RB1, ISG15, STAT1, IRF8, CYBB* and *NEMO*) defining 17 different genetic etiologies have been identified to date.[4-11] Mutations of *IL12B, IL12RB1* and *NEMO* impair the production of interferon (IFN)-γ, whereas mutations of *IFNGR1, IFNGR2* and *STAT1* impair cellular responses to IFN-γ. Moreover, autosomal recessive (AR) ISG15 deficiency has recently been identified as a genetic cause of MSMD.[11] A lack of ISG15 secretion by leukocytes results in impaired IFN-γ production by NK and T lymphocytes, accounting for mycobacterial disease. Thus, single-gene variants disrupting IL-12- or ISG15-dependent, IFN-γ-mediated immunity result in an inherited predisposition to mycobacterial infections.[12,13] However, no genetic etiology has yet been established for about half the patients with MSMD.

The first identification of MSMD-causing mutations of *STAT1* in 2001 was surprising, because STAT1 is involved in cellular responses mediated by cytokines other than IFN-γ, including IFN-α/β in particular. IFN-γ stimulation results in the phosphorylation of STAT1 on tyrosine 701, inducing its homodimerization to form gamma-activated factor (GAF). GAF binds the gamma-activated sequence (GAS) to induce the transcription of target genes involved in antimycobacterial immunity. On the other hand, IFN-α/β stimulation induces the phosphorylation of both STAT1 and STAT2, resulting in the formation of the heterotrimeric IFN-stimulated gene factor-3 (ISGF3) complex with IRF9. ISGF3 recognizes IFN-stimulated response element (ISRE) motifs in target genes and their expression confers anti-viral immunity. Indeed, heterozygosity for STAT1 dominant-negative alleles is responsible for AD MSMD.[14-17] Six mutations, *E320Q, Q463H, K637E, M654K, K673R* and *L706S* in *STAT1*, have been reported (Figure 1A).[14-17] The L706S mutation affects the tail segment domain of STAT1, abolishing phosphorylation at Y701.[14] The E320Q and Q463H mutations affect the DNA-binding domain.[15] They have no effect on STAT1 phosphorylation, but modify the DNA-binding capacity of GAF, impairing

 doi:10.3324/haematol.2013.083741
OH and SO contributed equally to this manuscript.
The online version of this article has a Supplementary Appendix.
Manuscript received on January 6, 2013. Manuscript accepted on April 5, 2013.
Correspondence: masak@hiroshima-u.ac.jp

STAT1-dependent immunity. The other three mutations affect the SH2 domain. The M654K and K673R mutations impair the tyrosine phosphorylation of STAT1, whereas the K637E mutation impairs both STAT1 phosphorylation and GAF-DNA binding.[16,17] These mutations are loss-of-function or hypomorphic and have been shown to exert a dominant-negative effect on wild-type STAT1 for IFN-γ responses.[14,15] We report here the molecular and clinical features of a multiplex kindred with MSMD due to a new *STAT1* allele, with a mutation of the tyrosine 701 codon.

Methods

Case report

The patient (P1) is a 5-year old Japanese boy born to a non-consanguineous family (Figure 1B). At the age of 2 months he presented with a mild fever and rash. Initial laboratory tests demonstrated leukocytosis (28.9x10^9/L) with eosinophilia (11.1x10^9/L) and a mild acute-phase inflammatory response. Treatment with cefotaxime was initiated and the patient's symptoms improved over the first 2 days, but leukocytosis with eosinophilia persisted for 2 weeks. No bacteria could be cultured from blood, the pharynx or stool samples. P1 was vaccinated with BCG at the age of 4 months. At the age of 3 years, he suffered severe back pain and dysbasia. Laboratory tests revealed mild leukocytosis (13.9x10^9/L) and high levels of C-reactive protein (3.99 mg/dL) and immunoglobulin (IgG; 2070 mg/dL) in the serum. Magnetic resonance imaging and whole-body bone scintigraphy revealed multifocal osteomyelitis in three vertebrae and the cranial, costal, clavicular, bilateral tibial and pelvic bones. Histological findings for the tibial bone were suggestive of tuberculoid granulomas, but no pathogenic bacteria, including *Mycobacterium*, were detected in the tissues by polymerase chain reaction or culture. The patient's leukocytes displayed a normal oxidative burst and normal proliferation in response to stimulation with phytohemagglutinin and concanavalin A. *STAT1* sequencing revealed a heterozygous nucleotide substitution (2102 A>G) in exon 23, resulting in the substitution of a cysteine for a tyrosine residue at amino-acid position 701 (Y701C). The patient (P1) started treatment with antimycobacterial drugs, including rifampicin, sulfamethoxazole/trimethoprim and clarithromycin. The clinical symptoms and laboratory parameters responded well to the treatment. These treatments have been maintained ever since, with the patient now being 5 years old. The patient has had no episodes of severe viral infection. He has had mumps, chicken pox and flu, but all these diseases followed a normal clinical course. Normal levels of specific antibodies against these viruses were detected in P1 (*Online Supplementary Table S1*). He has not yet been vaccinated against measles and rubella.

His mother (P2) was vaccinated with BCG in infancy without complications. She had a history of multifocal osteomyelitis in the frontal bone, right maxilla, multiple vertebral bodies and ribs at 18 years of age. Initial laboratory tests showed a moderate acute-phase inflammatory response. Histological findings in the costal bone were consistent with a granulomatous change. No pathogenic bacteria were detected. P2 was treated with levofloxacin hydrate and loxoprofen for 2 years. These treatments improved, but did not cure the symptoms. After this episode, P2 suffered from recurrent cervical and back pain. At the age of 38, confluent changes in the pressure on cervical and lumbar vertebrae were detected on plain X ray, as a sequel of multifocal osteomyelitis. Since the identification of a heterozygous Y701C *STAT1* mutation in the family study, P2 has been treated with rifampicin, sulfamethoxazole/trimethoprim and clarithromycin. This treatment appears to be effective, as the recurrent bone pain disappeared after treatment initiation. P2 presented no signs suggestive of immunodeficiency during childhood. She had no history of severe viral infections and normal levels of the specific antibodies against Epstein-Barr, chicken pox, mumps, rubella and measles viruses (*Online Supplementary Table S1*).

We obtained blood samples from the patients, relatives, and healthy adult controls, after obtaining informed consent. This study was approved by the Ethics Committee/Internal Review Board of Hiroshima University.

The experimental methods are described in detail in the *Online Supplementary Methods* section.

Results

Identification of a new STAT1 mutation

High-molecular weight genomic DNA was extracted from peripheral blood. The exons and the flanking introns of genes responsible for MSMD, including *STAT1*, *IFNGR1*, *IFNGR2*, *IL12B*, *IL12RB1* and *NEMO*, were amplified by PCR and analyzed by Sanger sequencing. We identified a new heterozygous mutation, 2102 A>G (Y701C), in exon 23 of *STAT1* in P1 (Figure 1B). The Y701C mutation was not found in the National Center for Biotechnology Information, Ensembl or dbSNP databases, or in our own in-house database of 621 exomes. We also sequenced *STAT1* in 1,052 controls from 52 ethnic groups from the *Centre d'Etude du Polymorphisme Humain* and Human Genome Diversity panels; Y701C was not detected in these controls. This mutation was therefore considered to be a rare variant rather than an irrelevant polymorphism. Familial segregation analysis identified the same mutation in the subject's mother (P2), whereas the father and older brother were both wild-type and healthy. The mother had a history of multiple osteomyelitis of unknown etiology at 18 years of age, revealing an AD pattern of segregation of the MSMD clinical phenotype with heterozygosity for the *STAT1* allele. Figure 1A shows previously identified heterozygous or biallelic *STAT1* mutations causing AD or AR genetic susceptibility to mycobacterial diseases.[14-22] The Y701C mutation affects the Y701 residue, the site of tyrosine phosphorylation in the STAT1 tail segment domain, a residue crucial for the activation of this molecule.[23,24]

STAT1 phosphorylation and cytokine production by peripheral blood mononuclear cells in response to interferon-γ stimulation

Interferon-γR1 is expressed ubiquitously, at moderate levels, on the cell surface, whereas very little IFN-γR2 is present and the expression of this receptor is tightly regulated, both spatially and temporally. Thus, IFN-γR2 is thought to be the factor determining responsiveness to IFN-γ.[25-27] The CD14-positive monocytes in peripheral blood are known to express relatively high levels of IFN-γR2.[28] We, therefore, investigated the cellular response to IFN-γ, focusing on CD14-positive monocytes. We purified CD14-positive monocytes by magnetic sorting and incubated them in the presence of lipopolysaccharide and various concentrations of IFN-γ. We then collected the supernatant, in which we determined tumor necrosis factor (TNF) levels. TNF production was severely impaired in the patients (P1 and P2), regardless of the dose of IFN-γ used for stimulation (Figure 1C). We analyzed STAT1 phospho-

rylation in response to IFN-γ by flow cytometry. STAT1 phosphorylation levels were lower in CD14-positive monocytes from patients than in control cells (Figure 1D). The CD14-positive monocytes of both patients displayed severe impairment of TNF production in the presence of lipopolysaccharide and IFN-γ, probably due to the impairment of Y701 phosphorylation in response to IFN-γ stimulation.

STAT1 phosphorylation and DNA-binding ability in Epstein-Barr virus-B cells

We assessed STAT1 production and phosphorylation in

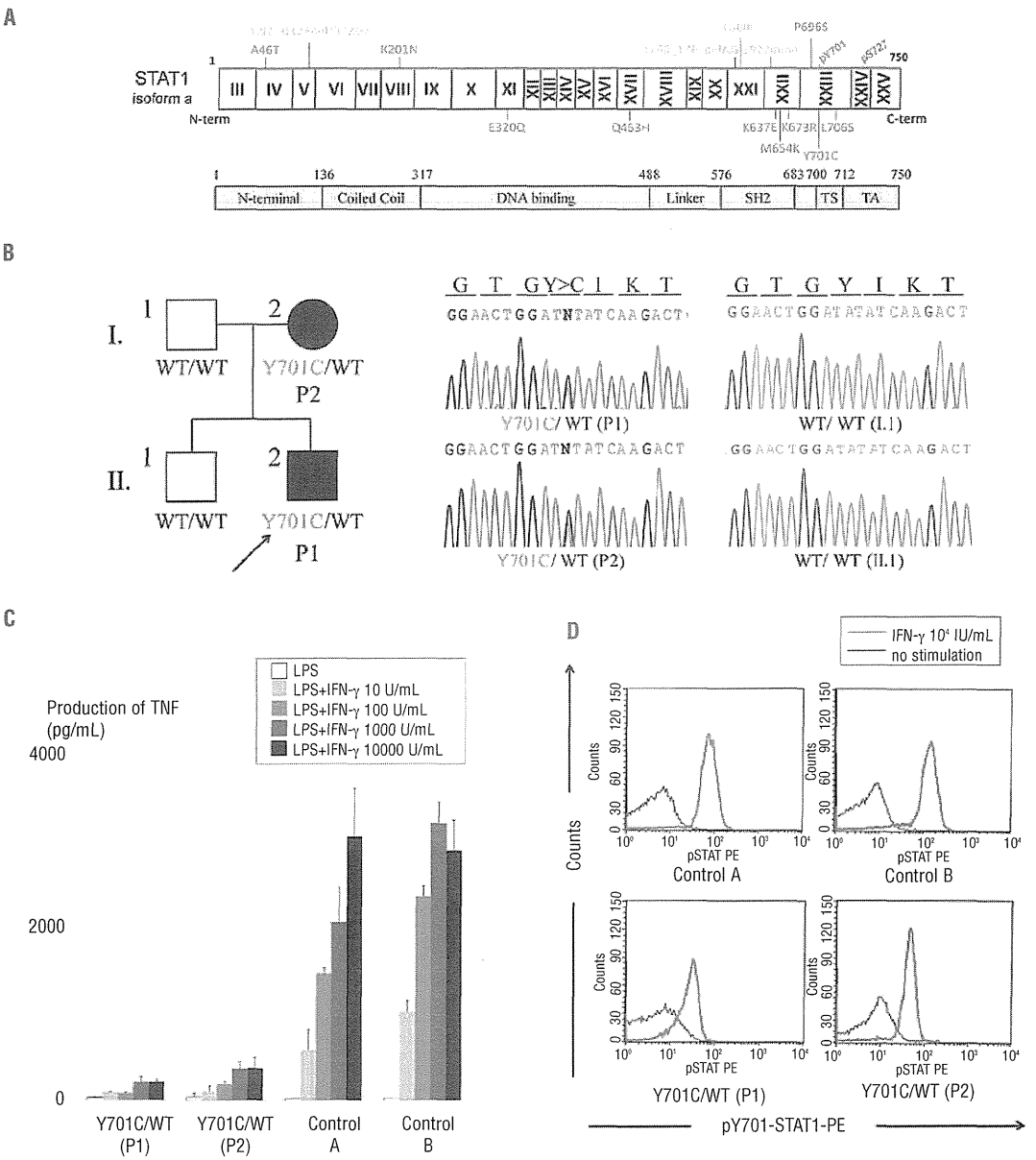

Figure 1. (A) Summary of loss-of-function *STAT1* mutations. The N-terminal domain, coiled-coil domain, DNA-binding domain, linker domain, SH2 domain, tail segment domain (TS), and transactivation domain (TA) are shown, together with Y701, the site of tyrosine phosphorylation. The dominant-negative mutants (blue) are indicated below the protein and the recessive forms of hypomorphic (green) and loss-of-function mutations (yellow) are shown above the protein. Y701C is shown in red. (B) The heterozygous Y701C mutation was detected in the patient (II.2) and his mother (I.2). Closed symbols indicate an affected individual and open symbols indicate a healthy family member. (C) CD14-positive monocytes were incubated in the presence of lipopolysaccharide (LPS) (100 ng/mL) and various concentrations of IFN-γ for 48 h and TNF production was then analyzed. CD14-positive monocytes from the patients (P1 and P2) produced abnormally small amounts of TNF. Two independent experiments were performed. (D) Flow cytometry analysis of STAT1 phosphorylation upon IFN-γ stimulation, on peripheral monocytes (CD14⁺ gate). STAT1 phosphorylation levels were lower in the patients' cells than in control cells. The black line indicates an absence of stimulation and the red line, stimulation with 10^4 IU/mL IFN-γ. Three independent experiments were performed.

Epstein-Barr virus (EBV)-B cells from a healthy control (WT/WT), P1 (Y701C/WT), another patient with AD STAT1 deficiency (L706S/WT) and a patient with complete STAT1 deficiency (1760_1761delAG/1760_1761delAG, -/-), by immunoblotting (Figure 2A).[14,20,21] STAT1 protein levels were normal in all EBV-B cells except those from a patient with complete STAT1 deficiency. However, STAT1 phosphorylation in response to stimulation with interferons was weak, but not abolished, in EBV-B cells carrying Y701C or L706S mutations. The DNA-binding ability of the mutant STAT1 proteins was analyzed by electrophoretic mobility shift assay on EBV-B cells. EBV-B cells containing the Y701C or L706S STAT1 proteins displayed a partial impairment of GAF DNA-binding in response to stimulation with interferons (Figure 2C). The GAF-DNA binding complexes were shown, by supershift analysis, to consist of STAT1 homodimers, STAT3 homodimers and STAT1/3 heterodimers, following stimulation with IFN-γ and IFN-α, respectively (*data not shown*). As previously described, GAF was unable to bind DNA in response to IFN-γ in EBV-B cells from a patient with complete STAT1 deficiency.[20] However, a complex identified as STAT3 homodimers was visible following incubation with IFN-α. By contrast, ISRE binding to DNA following IFN-α stimulation was found to be similar in cells from the patients and cells from controls, except for complete STAT1 deficiency. STAT1 phosphorylation and GAF DNA binding in EBV-B cells were impaired to a similar extent in P1 and P2 (*Online Supplementary Figure S1B,C*). Overall, EBV-B cells from the patients displayed impaired, but not abolished, STAT1 phosphorylation in response to stimulation with interferons, resulting in the partial impairment of GAF-DNA binding. However, ISRE-DNA binding levels in response to IFN-α stimulation were unaffected.

The phosphorylation and nuclear translocation of Y701C STAT1 are impaired

We transiently introduced WT and mutant *STAT1* into U3C cells by lipofection, and analyzed, by immunoblotting, the tyrosine 701 phosphorylation of the resulting protein in response to stimulation with IFN-α or IFN-γ (Figure 2B). Both Y701C and L706S STAT1 proteins impaired phosphorylation. As previously reported, the

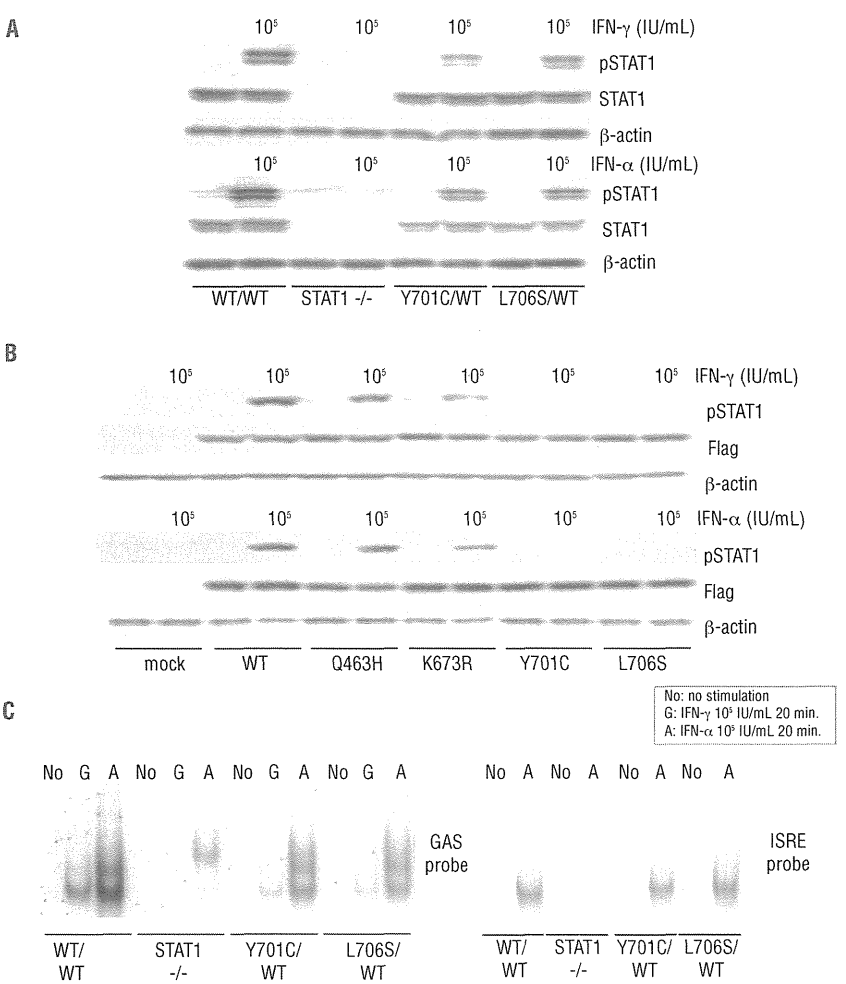

Figure 2. **STAT1 phosphorylation and DNA-binding ability in EBV-B cells. STAT1 production and phosphorylation in EBV-B cells (A) and transiently transfected U3C cells (B). The cells were stimulated with 10^5 IU/mL IFN for 15 min and subjected to immunoblot analysis. (A) EBV-B cells carrying heterozygous Y701C or L706S mutations showed a marked impairment of phosphorylation. The level of pSTAT1 was decreased in Y701C or L706S carrying cells by as much as 50.0% or 57.6% after IFN-γ stimulation and up to 66.3 % or 61.5 % after IFN-α stimulation when compared with healthy controls. (B) The Q463H STAT1 protein was normally phosphorylated, to levels similar to those observed for the WT protein. K673R STAT1 was only weakly phosphorylated. The Y701C STAT1 protein was not phosphorylated. (C) DNA-binding ability in EBV-B cells, as assessed by electrophoretic mobility shift assay with GAS and ISRE probes. EBV-B cells carrying Y701C or L706S mutations displayed a marked impairment of GAF DNA-binding ability. This impairment was particularly strong after IFN-γ stimulation. The ability of ISGF3 to bind DNA upon stimulation with IFN-α was preserved at almost normal levels in the patients' cells. At least two independent experiments were performed. (G: 10^5 IU/mL IFN-γ, A: 10^5 IU/mL IFN-α)**

phosphorylation of K673R STAT1 was partially impaired.[16] By contrast, the Q463H STAT1 mutant was phosphorylated to almost the same degree as the WT protein. We then analyzed the nuclear translocation of STAT1 in U2OS cells stably expressing flag-tagged WT, Q463H, K673R, L706S and Y701C STAT1 mutant alleles. Unphosphorylated STAT1 was mostly present in the cytoplasm before IFN-γ stimulation (*Online Supplementary Figure S2A*). After IFN-γ stimulation, STAT1 was found in the nucleus in cells producing the WT and Q463H STAT1 proteins (*Online Supplementary Figure S2B*). By contrast, STAT1 nuclear translocation was severely impaired in cells producing the Y701C and L706S STAT1 proteins. The K673R mutant STAT1 protein was present in both the nucleus and the cytoplasm, suggesting incomplete nuclear translocation. These results suggest that the Y701C mutation, like L706S, prevents STAT1 phosphorylation and nuclear translocation.

Comparison of the Y701C and L706S mutations

Both the Y701C and L706S mutations affect residues in the tail segment domain of STAT1. We focused on these two mutations and performed further functional characterization. We treated cells carrying these mutations with the tyrosine phosphatase inhibitor pervanadate and then analyzed the phosphorylation of STAT1 upon IFN-γ stimulation.[29] STAT1 phosphorylation was restored in the presence of pervanadate in cells carrying the L706S mutation, whereas no such restoration was observed for the Y701C mutant (Figure 3A). Conversely, pervanadate treatment did not rescue GAF-DNA binding for L706S STAT1 (Figure 3A). We investigated the mechanisms underlying these experimental observations by extracting the cytosol and investigating STAT1 phosphorylation by immunoblotting (Figure 3B). The L706S STAT1 protein showed almost normal levels of phosphorylation in the cytosol fraction after pervanadate treatment, whereas

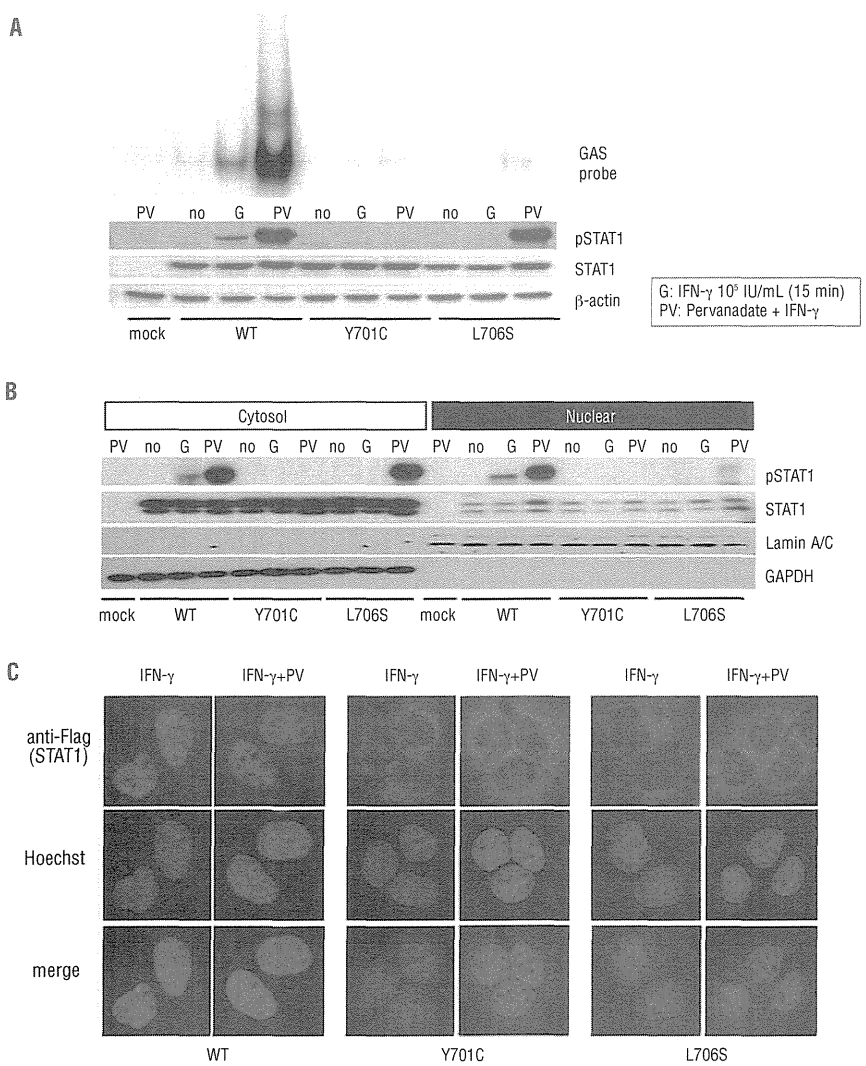

Figure 3. **Comparison of the Y701C and L706S mutations.** (A) **U3C transfectants were stimulated with 10^5 IU/mL IFN-γ in the presence or absence of pervanadate for 15 min and subjected to immunoblotting and electrophoretic mobility shift assay. The L706S STAT1 protein was phosphorylated to almost normal levels in response to IFN-γ stimulation in the presence of pervanadate, whereas no phosphorylation of the Y701C STAT1 protein was observed. However, L706S STAT1 was still associated with a lack of GAF-DNA binding, even after its phosphorylation had been restored.** (B) **STAT1 phosphorylation was investigated in the nuclear and cytosolic fractions, by immunoblotting. The phosphorylated L706S STAT1 protein was mostly present in the cytosol fraction.** (C) **U2OS cells stably expressing Flag-tagged WT, Y701C, or L706S STAT1 were stimulated with IFN-γ for 30 min in the presence or absence of pervanadate and subjected to immunostaining. Nuclear translocation was severely impaired in cells producing either Y701C or L706S STAT1, even after pervanadate treatment. At least two independent experiments were carried out.**

phosphorylation was severely impaired in the nuclear fraction. These results suggest that the L706S mutation impairs both phosphorylation and nuclear translocation. This impairment of the nuclear translocation of L706S STAT1 was confirmed by immunostaining (Figure 3C). The L706S mutant protein was, therefore, considered to have at least two molecular defects: severe impairments of both phosphorylation and the nuclear translocation of STAT1. By contrast, Y701C STAT1 phosphorylation was totally abolished and could not be restored by pervanadate treatment.

Transcriptional activity of the mutant STAT1 proteins

We investigated the impact of the STAT1 Y701C mutation on the transcriptional activities of GAS and ISRE, by carrying out reporter assays with GAS or ISRE reporter plasmids. Production of the Y701C and L706S STAT1 proteins was associated with abolition of the transcriptional activities of both GAS and ISRE (*Online Supplementary Figure S3A,C*). Co-transfection experiments revealed that these mutant proteins had negative effects on the WT protein in GAS transcriptional activity (*Online Supplementary Figure S3B*). Furthermore, a dose-dependent negative-dominance effect was clearly observed for the Y701C and L706S mutant proteins. By contrast, ISRE transcriptional activity remained at almost normal levels in cells co-transfected with the L706S plasmid (*Online Supplementary Figure S3D*). The level of ISRE transcriptional activity was repeatedly found to be lower with Y701C STAT1, but no clear dominant-negative effect was detected. These results are consistent with the results we observed in an electrophoretic mobility shift assay using EBV-B cells. Thus, the Y701C STAT1 allele has a dominant-negative effect, decreasing GAS activation but not ISRE activation.

Downstream gene induction in CD14-positive monocytes and Epstein-Barr virus-B cells

The induction of downstream interferon-stimulated genes (ISG) has been investigated with EBV-B cells from patients and in gene expression experiments using U3C cells.[15] We investigated the impact of the Y701C mutation further, by studying the induction of ISG in CD14-positive monocytes from patients, comparing the results obtained with those for EBV-B cells. We first purified CD14-positive monocytes, stimulated them with IFN-γ and analyzed the expression of the downstream ISG encoding *CXCL9* and *IRF1*, by real-time quantitative PCR analysis. Strong induction of *CXCL9* was observed at late time points (6 hours) in healthy controls, but this induction was severely impaired in the patients' cells (Figure 4A). In contrast, IRF1 induction was observed at both early and late time points. The patients' cells displayed a mild but significant impairment of *IRF1* induction at late time points, whereas the difference observed at early time points was not statistically significant. We then investigated the induction of *CXCL9*, *IRF1* and *ISG15* in EBV-B cells. The induction of these three ISG was STAT1-dependent, as shown by the abolition of induction in STAT1-null EBV-B cells. EBV-B cells carrying heterozygous Y701C or L706S mutations displayed severely impaired induction of *CXCL9* and *ISG15* in response to interferons (Figure 4B,C). Unlike CD14-positive monocytes, the peak of *IRF1* induction was observed at early time points in EBV-B cells. The impairment of *IRF1* induction was mild and mostly observed at early time points in EBV-B cells from the patients. Thus, CD14-positive monocytes and EBV-B cells behaved similarly, but not identically, in terms of ISG induction in response to IFN-γ stimulation. These results suggest that the induction of ISG is impaired in the patients' cells.

Discussion

We report here a novel heterozygous *STAT1* mutation, 2102 A>G (Y701C), which results in STAT1 deficiency and AD MSMD. The Y701 residue serves as a site of phosphorylation for STAT1, this phosphorylation playing a key role in STAT1-mediated signal transduction. Indeed, AD *STAT1* mutations impairing STAT1 phosphorylation have been shown to underlie the pathogenesis of MSMD.[14-17] Furthermore, AD mutations that cause gains of phosphorylation because they impair the nuclear dephosphorylation of STAT1 have been identified in patients with chronic mucocutaneous candidiasis.[30-34] The Y701C mutant STAT1 protein displayed a complete abolition of Y701 phosphorylation and downstream events, such as the nuclear translocation and transcriptional activities of GAS and ISRE. The Y701C *STAT1* allele is dominant for GAF, but recessive for ISGF3. This observation is highly consistent with previously identified STAT1 mutations in patients with AD STAT1 deficiencies and the molecular mechanisms can be explained by differences in the structure of GAS (homodimer of STAT1) and ISGF3 (heterodimer of STAT1/STAT2/IRF9).[14-17] The Y701C mutation is thus responsible for MSMD without viral disease. Two heterozygous *STAT1* mutations, Y701C and L706S, affect residues located in the same tail segment domain and result in the impairment of Y701 phosphorylation. However, these two mutants responded differently to stimulation in the presence of pervanadate. This treatment rescued Y701 phosphorylation in L706S STAT1, but not in the Y701C protein. The functional defect seemed to be more severe for the Y701C than for the L706S mutant protein, as shown by GAS reporter assays and real-time quantitative PCR analysis. The Y701C mutation may therefore have a stronger negative impact *in vitro* than L706S *STAT1*. However, in contrast to the findings of these *in vitro* studies, the clinical symptoms of the patient and his mother were similar to those of previously identified patients with AD STAT1 deficiency.

We also investigated the induction of ISG upon IFN-γ stimulation in CD14-positive monocytes from the patients. ISG induction has been intensively investigated in EBV-B cells,[15,17] but this is the first study to investigate the induction of ISG in primary cells from patients. Both EBV-B cell lines and primary monocytes from the patients showed severe impairment of *CXCL9* induction. Minor differences in induction patterns were observed, but both types of cell showed mild impairment of *IRF1* induction. Thus, the impairment of ISG induction was confirmed not only in EBV-B cells, but also in the patients' monocytes. IL-12p40 induction is totally dependent on Irf1 in mice.[35-37] Macrophages from *Irf1*-null mice display impaired induction of inducible nitric oxide synthase in response to lipopolysaccharide.[38,39] Furthermore, *Irf1*-null mice develop severe symptoms when infected with *Mycobacterium bovis*. Thus, the impairment of *IRF1* induction observed in CD14-positive monocytes may contribute to host susceptibility to mycobacteria. We also observed an impairment in *ISG15* induction in the patients' EBV-B cells. The recent

identification of ISG15 deficiency in some human patients with MSMD has provided evidence of an important role for this molecule in host immunity to mycobacteria.[11] Heterozygous *STAT1* mutations thus have negative effects on the downstream induction of ISG involved in host defense against mycobacteria, and this *in vitro* cellular phenotype is commonly observed in the patients' cells. However, the magnitude of this negative impact may dif-

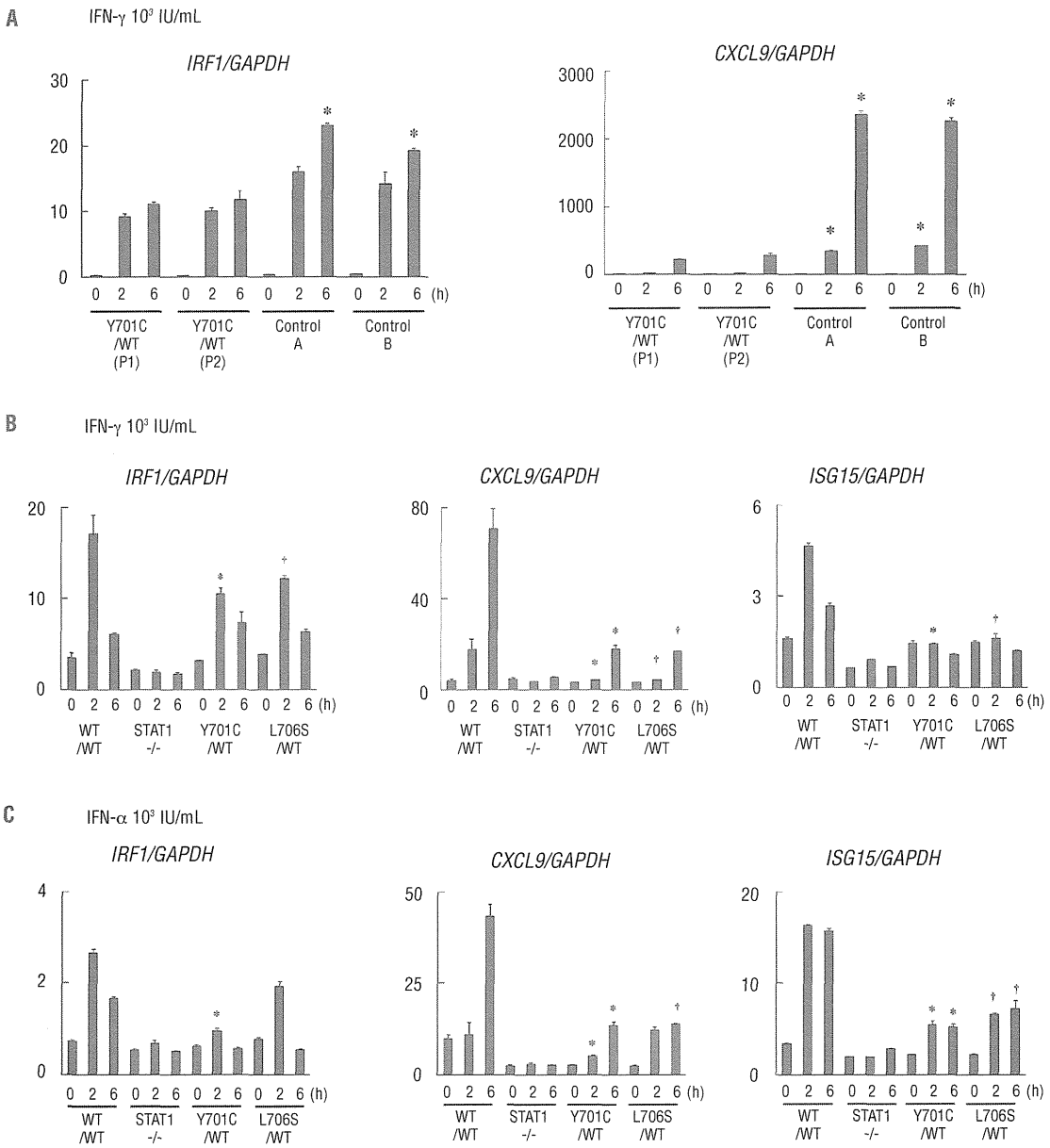

Figure 4. **Analysis of gene expression. The induction of ISG was analyzed by real-time quantitative PCR.** (A) **CD14-positive monocytes from the patients (P1, P2) and two healthy controls were stimulated with 10^3 IU/mL IFN-γ (for 2 or 6 h) and the induction of *CXCL9* and *IRF1* was investigated. The induction of *CXCL9* was severely impaired in the patients' cells, whereas the induction of *IRF1* was only mildly impaired. *Differences were statistically significant in monocytes from the patients compared with those from healthy individuals (*P*<0.05).** (B, C) **The induction of *CXCL9*, *IRF1* and *ISG15* in EBV-B cells from the patients, Y701C/WT and L706S/WT cells, and cells from healthy individuals, in response to IFN-γ** (B) **or IFN-α** (C) **stimulation. EBV-B cells carrying Y701C or L706S mutations displayed severe impairment of *CXCL9* induction in response to IFN stimulation. The induction of *IRF1* and *ISG15* was also impaired, but to a lesser extent than that of *CXCL9*. ISG expression was normalized with respect to *GAPDH*. The results shown are representative of three independent experiments, except for the CD14⁺ monocyte experiment (which was performed twice). Differences were statistically significant between cells carrying either the Y701C mutation *(*P*<0.05) or L706S mutation †(*P*<0.05) and EBV-B cells from healthy individuals.**

fer between cell types and between the ISG induced. The induction of ISG has also been intensively investigated in patients with AR STAT1 deficiency.[22] As in the current study, the severity of impairment differed in the patient's cells depending on the ISG induced. These observations reflect the complexity of STAT1-mediated signaling.[40]

Including the two patients studied here, 11 patients with AD STAT1 deficiency have been identified to date. Five of these 11 patients have developed multifocal osteomyelitis, a typical clinical feature of patients with AD partial IFN-γR1 deficiency.[4,41] Our initial patient had multifocal osteomyelitis showing tuberculoid granulomas without the detection of pathogenic mycobacterium by culture and/or PCR amplification. Additionally, his mother had a history of multifocal osteomyelitis. These observations emphasize the importance of multifocal osteomyelitis as one of the representative clinical manifestation even in patients with AD STAT1 deficiency. We have summarized the clinical manifestations of 11 patients with AD STAT1 deficiency,[14-17] 53 patients with AD partial IFN-γR1 deficiency,[41-45] 14 patients with AR partial IFN-γR1 deficiency[46] and 102 patients with AR IL-12Rβ1 deficiency,[47] the most common genetic etiology of MSMD (Table 1). The frequency of multifocal osteomyelitis was high in AD STAT1 deficiency (45.5%), AD partial IFN-γR1 deficiency (79.2%) and AR partial IFN-γR1 deficiency (50.0%), but lower in patients with AR complete IFN-γR1 deficiency (13%).[41] Unfortunately, this clinical manifestation has not been investigated in patients with AR IL-12Rβ1 deficiency.[47] In many cases, either BCG or environmental mycobacteria have been proven to be present by biopsy of osteomyelitis. By contrast, the frequency of BCG disease, a common sign in patients with MSMD, in patients vaccinated with BCG is similar to that in AD STAT1 deficiency (77.8%), AD partial IFN-γR1 deficiency (76.7%), AR partial IFN-γR1 deficiency (85.7%) and AR IL-12Rβ1 deficiency (77.9%). The clinical signs of AD STAT1 deficiency may, therefore, be considered to be similar to those of partial IFN-γR1 deficiency. There are several possible reasons for this: (i) STAT1 is a non-redundant downstream transcription factor for IFN-γ signaling;[4] (ii) STAT1 mutations impair GAF-mediated signaling, but not ISGF3-mediated signaling, and IFN-γ induces GAF, but not ISGF3;[48] (iii) IFN-γ signaling is only partially impaired in both disorders.[4] The clinical similarities between these two disorders support our hypothesis that the symptoms accompanying AD STAT1 deficiency result from an impairment of cellular responses to IFN-γ. Multifocal osteomyelitis is a characteristic symptom common to three different disorders: AD partial IFN-γR1 deficiency, AR partial IFN-γR1 deficiency and AD STAT1 deficiency. Multifocal osteomyelitis should, therefore, lead to investigations of both STAT1 and IFN-γR1.

Table 1. **Comparison of clinical manifestations.**

	AD STAT1 deficiency	AD partial IFN-γR1 deficiency	AR partial IFN-γR1 deficiency	AR IL-12Rβ1 deficiency
N. of cases	11	53	14	102
Onset of MSMD	5.3y (0.5y-18y)	10.8y (0.1y-62y)	11.2y (0.1y-31y)	2.4y (0.1y-31y)
BCG disease (among vaccinated patients)	7/9	23/30	6/7	67/86
Environmental mycobacteria	5/11	42/53	6/14	19/102
M. tuberculosis complex		2/53	1/14	5/102
Salmonella spp.	none	2/53	3/14	44/102
Severe viral infection	none	1/53	none	none
Osteomyelitis	5/11	42/53	7/14	
Locations of mycobacterial infections				
Nodes	2/11	30/53		6/14
Other organs	4/11	11/53		6/14
References	*14-17*	*41-45*	*46*	*47*

Acknowledgments

The authors would like to thank Xiao-Fei Kong, MD, PhD, Vanessa Bryant, PhD, Dusan Bogunovic, PhD, Alexandra Kreins, MD, Marcela Moncada-Velez, BSc, Michael Ciancaneli, PhD, and Avinash Abhyankar, MD, PhD, for helpful discussions and critical reading. We also thank the members of the laboratory, Yelena Nemirovskaya and Eric Anderson for secretarial assistance, and Tiffany Nivare for technical assistance. Sequence analysis support was provided by the Analysis Center of Life Science, Natural Science Center for Basic Research and Development, Hiroshima University.

Funding

This study was supported, in part, by Grants in Aid for Scientific Research from the Japan Society for the Promotion of Science [22591161 to M.K.], and by Research on Measures for Intractable Diseases funding from the Japanese Ministry of Health, Labor and Welfare [H22-Nanchi-ippan-078 to MK]. This study was also supported, in part, by the Rockefeller University and grants from the National Center for Research Resources, and the National Center for Advancing Sciences (NCATS), National Institutes of Health (NIH) grant number 8UL1TR000043, NIH grant number R01AI089970, and the St. Giles Foundation. SC was supported by the AXA Research Fund and X-FK by the Stony Wold-Herbert Fund.

Authorship and Disclosures

Information on authorship, contributions, and financial & other disclosures was provided by the authors and is available with the online version of this article at www.haematologica.org.

References

1. Casanova JL, Abel L. Genetic dissection of immunity to mycobacteria: the human model. Annu Rev Immunol. 2002;20:581-620.
2. Hamosh A, Scott AF, Amberger JS, Bocchini CA, McKusick VA. Online Mendelian Inheritance in Man (OMIM), a knowledgebase of human genes and genetic disorders. Nucleic Acids Res. 2005;33(Database issue):D514-7.
3. Alcais A, Fieschi C, Abel L, Casanova JL. Tuberculosis in children and adults: two distinct genetic diseases. J Exp Med. 2005;202(12):1617-21.
4. Filipe-Santos O, Bustamante J, Chapgier A, Vogt G, de Beaucoudrey L, Feinberg J, et al. Inborn errors of IL-12/23- and IFN-gamma-mediated immunity: molecular, cellular, and clinical features. Semin Immunol. 2006;18(6):347-61.
5. Vogt G, Bustamante J, Chapgier A, Feinberg J, Boisson Dupuis S, Picard C, et al. Complementation of a pathogenic IFNGR2 misfolding mutation with modifiers of N-glycosylation. J Exp Med. 2008;205(8):1729-37.
6. Bustamante J, Arias AA, Vogt G, Picard C,

Galicia LB, Prando C, et al. Germline CYBB mutations that selectively affect macrophages in kindreds with X-linked predisposition to tuberculous mycobacterial disease. Nat Immunol. 2011;12(3):213-21.
7. Hambleton S, Salem S, Bustamante J, Bigley V, Boisson-Dupuis S, Azevedo J, et al. IRF8 mutations and human dendritic-cell immunodeficiency. N Engl J Med. 2011;365(2):127-38.
8. Al-Muhsen S, Casanova JL. The genetic heterogeneity of mendelian susceptibility to mycobacterial diseases. J Allergy Clin Immunol. 2008;122(6):1043-51; quiz 52-3.
9. Boisson-Dupuis S, Kong XF, Okada S, Cypowyj S, Puel A, Abel L, et al. Inborn errors of human STAT1: allelic heterogeneity governs the diversity of immunological and infectious phenotypes. Curr Opin Immunol. 2012;24(4):364-78.
10. Casanova JL, Holland SM, Notarangelo LD. Inborn errors of human JAKs and STATs. Immunity. 2012;36(4):515-28.
11. Bogunovic D, Byun M, Durfee LA, Abhyankar A, Sanal O, Mansouri D, et al. Mycobacterial disease and impaired IFN-gamma immunity in humans with inherited ISG15 deficiency. Science. 2012;337(6102):1684-8.
12. Casanova JL, Abel L. Inborn errors of immunity to infection: the rule rather than the exception. J Exp Med. 2005;202(2):197-201.
13. Alcais A, Quintana-Murci L, Thaler DS, Schurr E, Abel L, Casanova JL. Life-threatening infectious diseases of childhood: single-gene inborn errors of immunity? Ann NY Acad Sci. 2010;1214:18-33.
14. Dupuis S, Dargemont C, Fieschi C, Thomassin N, Rosenzweig S, Harris J, et al. Impairment of mycobacterial but not viral immunity by a germline human STAT1 mutation. Science. 2001;293(5528):300-3.
15. Chapgier A, Boisson-Dupuis S, Jouanguy E, Vogt G, Feinberg J, Prochnicka-Chalufour A, et al. Novel STAT1 alleles in otherwise healthy patients with mycobacterial disease. PLoS Genet. 2006;2(8):e131.
16. Tsumura M, Okada S, Sakai H, Yasunaga S, Ohtsubo M, Murata T, et al. Dominant-negative STAT1 SH2 domain mutations in unrelated patients with Mendelian susceptibility to mycobacterial disease. Hum Mutat. 2012;33(9):1377-87.
17. Sampaio EP, Bax HI, Hsu AP, Kristosturyan E, Pechacek J, Chandrasekaran P, et al. A novel STAT1 mutation associated with disseminated mycobacterial disease. J Clin Immunol. 2012;32(4):681-9.
18. Kristensen IA, Veirum JE, Moller BK, Christiansen M. Novel STAT1 alleles in a patient with impaired resistance to mycobacteria. J Clin Immunol. 2011;31(2):265-71.
19. Vairo D, Tassone L, Tabellini G, Tamassia N, Gasperini S, Bazzoni F, et al. Severe impairment of IFN-gamma and IFN-alpha responses in cells of a patient with a novel STAT1 splicing mutation. Blood. 2011;118(7):1806-17.
20. Dupuis S, Jouanguy E, Al-Hajjar S, Fieschi C, Al-Mohsen IZ, Al-Jumaah S, et al. Impaired response to interferon-alpha/beta and lethal viral disease in human STAT1 deficiency. Nat Genet. 2003;33(3):388-91.
21. Chapgier A, Wynn RF, Jouanguy E, Filipe-Santos O, Zhang S, Feinberg J, et al. Human complete Stat-1 deficiency is associated with defective type I and II IFN responses in vitro but immunity to some low virulence viruses in vivo. J Immunol. 2006;176(8):5078-83.
22. Kong XF, Ciancanelli M, Al-Hajjar S, Alsina L, Zumwalt T, Bustamante J, et al. A novel form of human STAT1 deficiency impairing early but not late responses to interferons. Blood. 2010;116(26):5895-906.
23. Shuai K, Ziemiecki A, Wilks AF, Harpur AG, Sadowski HB, Gilman MZ, et al. Polypeptide signalling to the nucleus through tyrosine phosphorylation of Jak and Stat proteins. Nature. 1993;366(6455):580-3.
24. Chen X, Vinkemeier U, Zhao Y, Jeruzalmi D, Darnell JE Jr, Kuriyan J. Crystal structure of a tyrosine phosphorylated STAT-1 dimer bound to DNA. Cell. 1998;93(5):827-39.
25. Bach EA, Aguet M, Schreiber RD. The IFN gamma receptor: a paradigm for cytokine receptor signaling. Annu Rev Immunol. 1997;15:563-91.
26. van Boxel-Dezaire AH, Stark GR. Cell type-specific signaling in response to interferon-gamma. Curr Top Microbiol Immunol. 2007;316:119-54.
27. Kong XF, Vogt G, Itan Y, Macura-Biegun A, Szaflarska A, Kowalczyk D, et al. Haploinsufficiency at the human IFNGR2 locus contributes to mycobacterial disease. Hum Mol Genet. 2013;22(4):769-81.
28. Bernabei P, Coccia EM, Rigamonti L, Bosticardo M, Forni G, Pestka S, et al. Interferon-gamma receptor 2 expression as the deciding factor in human T, B, and myeloid cell proliferation or death. J Leukoc Biol. 2001;70(6):950-60.
29. Tourkine N, Schindler C, Larose M, Houdebine LM. Activation of STAT factors by prolactin, interferon-gamma, growth hormones, and a tyrosine phosphatase inhibitor in rabbit primary mammary epithelial cells. J Biol Chem. 1995;270(36):20952-61.
30. Liu L, Okada S, Kong XF, Kreins AY, Cypowyj S, Abhyankar A, et al. Gain-of-function human STAT1 mutations impair IL-17 immunity and underlie chronic mucocutaneous candidiasis. J Exp Med. 2011;208(8):1635-48.
31. van de Veerdonk FL, Plantinga TS, Hoischen A, Smeekens SP, Joosten LA, Gilissen C, et al. STAT1 mutations in autosomal dominant chronic mucocutaneous candidiasis. N Engl J Med. 2011;365(1):54-61.
32. Smeekens SP, Plantinga TS, van de Veerdonk FL, Heinhuis B, Hoischen A, Joosten LA, et al. STAT1 hyperphosphorylation and defective IL12R/IL23R signaling underlie defective immunity in autosomal dominant chronic mucocutaneous candidiasis. PLoS One. 2011;6(12):e29248.
33. Takezaki S, Yamada M, Kato M, Park MJ, Maruyama K, Yamazaki Y, et al. Chronic mucocutaneous candidiasis caused by a gain-of-function mutation in the STAT1 DNA-binding domain. J Immunol. 2012;189(3):1521-6.
34. Toth B, Mehes L, Tasko S, Szalai Z, Tulassay Z, Cypowyj S, et al. Herpes in STAT1 gain-of-function mutation [corrected]. Lancet. 2012;379(9835):2500.
35. Taniguchi T, Ogasawara K, Takaoka A, Tanaka N. IRF family of transcription factors as regulators of host defense. Annu Rev Immunol. 2001;19:623-55.
36. Taki S, Sato T, Ogasawara K, Fukuda T, Sato M, Hida S, et al. Multistage regulation of Th1-type immune responses by the transcription factor IRF-1. Immunity. 1997;6(6):673-9.
37. Lohoff M, Ferrick D, Mittrucker HW, Duncan GS, Bischof S, Rollinghoff M, et al. Interferon regulatory factor-1 is required for a T helper 1 immune response in vivo. Immunity. 1997;6(6):681-9.
38. Kamijo R, Harada H, Matsuyama T, Bosland M, Gerecitano J, Shapiro D, et al. Requirement for transcription factor IRF-1 in NO synthase induction in macrophages. Science. 1994;263(5153):1612-5.
39. Martin E, Nathan C, Xie QW. Role of interferon regulatory factor 1 in induction of nitric oxide synthase. J Exp Med. 1994;180(3):977-84.
40. Gough DJ, Levy DE, Johnstone RW, Clarke CJ. IFNgamma signaling - does it mean JAK-STAT? Cytokine Growth Factor Rev. 2008;19(5-6):383-94.
41. Dorman SE, Picard C, Lammas D, Heyne K, van Dissel JT, Baretto R, et al. Clinical features of dominant and recessive interferon gamma receptor 1 deficiencies. Lancet. 2004;364(9451):2113-21.
42. Hoshina T, Takada H, Sasaki-Mihara Y, Kusuhara K, Ohshima K, Okada S, et al. Clinical and host genetic characteristics of mendelian susceptibility to mycobacterial diseases in Japan. J Clin Immunol. 2011;31(3):309-14.
43. Lee WI, Huang JL, Lin TY, Hsueh C, Wong AM, Hsieh MY, et al. Chinese patients with defective IL-12/23-interferon-gamma circuit in Taiwan: partial dominant interferon-gamma receptor 1 mutation presenting as cutaneous granuloma and IL-12 receptor beta1 mutation as pneumatocele. J Clin Immunol. 2009;29(2):238-45.
44. Glosli H, Stray-Pedersen A, Brun AC, Holtmon LW, Tonjum T, Chapgier A, et al. Infections due to various atypical mycobacteria in a Norwegian multiplex family with dominant interferon-gamma receptor deficiency. Clin Infect Dis. 2008;46(3):e23-7.
45. Okada S, Ishikawa N, Shirao K, Kawaguchi H, Tsumura M, Ohno Y, et al. The novel IFNGR1 mutation 774del4 produces a truncated form of interferon-gamma receptor 1 and has a dominant-negative effect on interferon-gamma signal transduction. J Med Genet. 2007;44(8):485-91.
46. Sologuren I, Boisson-Dupuis S, Pestano J, Vincent QB, Fernandez-Perez L, Chapgier A, et al. Partial recessive IFN-{gamma}R1 deficiency: genetic, immunological and clinical features of 14 patients from 11 kindreds. Hum Mol Genet. 2011;20(8):1509-23.
47. de Beaucoudrey L, Samarina A, Bustamante J, Cobat A, Boisson-Dupuis S, Feinberg J, et al. Revisiting human IL-12Rbeta1 deficiency: a survey of 141 patients from 30 countries. Medicine (Baltimore). 2010;89(6):381-402.
48. Ginter T, Bier C, Knauer SK, Sughra K, Hildebrand D, Munz T, et al. Histone deacetylase inhibitors block IFNgamma-induced STAT1 phosphorylation. Cell Signal. 2012;24(7):1453-60.

Wnt3a stimulates maturation of impaired neutrophils developed from severe congenital neutropenia patient-derived pluripotent stem cells

Takafumi Hiramoto[a,b], Yasuhiro Ebihara[b,c,1], Yoko Mizoguchi[d], Kazuhiro Nakamura[d], Kiyoshi Yamaguchi[e], Kazuko Ueno[f], Naoki Nariai[f], Shinji Mochizuki[b,c], Shohei Yamamoto[b,c], Masao Nagasaki[f], Yoichi Furukawa[e], Kenzaburo Tani[a], Hiromitsu Nakauchi[g], Masao Kobayashi[d], and Kohichiro Tsuji[b,c]

[a]Division of Molecular and Clinical Genomics, Medical Institute of Bioregulation, Kyushu University, Higashi-ku, Fukuoka 812-8582, Japan; [c]Department of Pediatric Hematology/Oncology, Research Hospital, Divisions of [b]Stem Cell Processing and [g]Stem Cell Therapy, Center for Stem Cell Biology and Regenerative Medicine, and [e]Division of Clinical Genome Research, Advanced Clinical Research Center, Institute of Medical Science, University of Tokyo, Minato-ku, Tokyo 108-8639, Japan; [d]Pediatrics, Hiroshima University Graduate School of Biomedical and Health Sciences, Minami-ku, Hiroshima 734-8551, Japan; and [f]Department of Integrative Genomics, Tohoku Medical Megabank Organization, Tohoku University, Aramaki, Aoba-ku, Sendai 980-8573, Japan

Edited by George Q. Daley, Children's Hospital Boston, Boston, MA, and accepted by the Editorial Board January 4, 2013 (received for review October 1, 2012)

The derivation of induced pluripotent stem (iPS) cells from individuals of genetic disorders offers new opportunities for basic research into these diseases and the development of therapeutic compounds. Severe congenital neutropenia (SCN) is a serious disorder characterized by severe neutropenia at birth. SCN is associated with heterozygous mutations in the neutrophil elastase [elastase, neutrophil-expressed (ELANE)] gene, but the mechanisms that disrupt neutrophil development have not yet been clarified because of the current lack of an appropriate disease model. Here, we generated iPS cells from an individual with SCN (SCN-iPS cells). Granulopoiesis from SCN-iPS cells revealed neutrophil maturation arrest and little sensitivity to granulocyte-colony stimulating factor, reflecting a disease status of SCN. Molecular analysis of the granulopoiesis from the SCN-iPS cells vs. control iPS cells showed reduced expression of genes related to the wingless-type mmtv integration site family, member 3a (Wnt3a)/β-catenin pathway [e.g., lymphoid enhancer-binding factor 1], whereas Wnt3a administration induced elevation lymphoid enhancer-binding factor 1-expression and the maturation of SCN-iPS cell-derived neutrophils. These results indicate that SCN-iPS cells provide a useful disease model for SCN, and the activation of the Wnt3a/β-catenin pathway may offer a novel therapy for SCN with ELANE mutation.

apoptosis | unfolded protein response | SCN disease model

Severe congenital neutropenia (SCN) is a heterogeneous bone marrow (BM) failure syndrome characterized by severe neutropenia at birth, leading to recurrent infections by bacteria or fungi (1). SCN patients reveal an arrest in neutrophil differentiation in the BM at the promyelocyte or myelocyte stage (1), as well as a propensity to develop myelodysplastic syndrome and acute myeloid leukemia (2). Current treatment by high-dose granulocyte-colony stimulating factor (G-CSF) administration induces an increase in the number of mature neutrophils in the peripheral blood of most SCN patients (3). Although this treatment is curative for the severe infections, there is a concern that high-dose G-CSF may increase the risk of hematologic malignancy in these individuals (4).

Several genetic mutations have been identified in SCN patients. Approximately 50% of autosomal-dominant SCN cases were shown to have various heterozygous mutations in the gene encoding neutrophil elastase [elastase, neutrophil-expressed (ELANE)] (5, 6), a monomeric, 218-amino acid (25 kDa) chymotryptic serine protease (7) that is synthesized during the early stages of primary granule production in promyelocytes (8, 9). However, the mechanism(s) causing impaired neutrophil maturation in SCN patients remains unclear due to the current lack of an appropriate disease model.

Results and Discussion

In the present study, we generated induced pluripotent stem (iPS) cells from the BM cells obtained from an SCN patient with a heterologous ELANE gene mutation (exon 5, 707 region, C194X) (SCN-iPS cells) to provide the basis for an SCN disease model. The patient who donated BM cells recurrently suffered from severe infections without exogenous G-CSF administration, but the G-CSF administration once a week prevented his repeated infection. The SCN-iPS cells continued to show embryonic stem cell morphology after >20 passages and also expressed pluripotent markers (Fig. S1*A*). The silencing of exogenous genes and the capability to differentiate into three germ layers by teratoma formation were confirmed for each of the three SCN-iPS cell clones (Fig. S1 *B* and *C*). Furthermore, the same ELANE gene mutation that was present in the patient persisted in the SCN-iPS cells (Fig. S1*D*). The SCN-iPS cells, as well as control iPS cells that were generated from healthy donors, had the normal karyotype (Fig. S1*E*) (10, 11) and no mutations in the mutation-sensitive region of the G-CSF receptor gene (12).

We first compared the hematopoietic differentiation from SCN-iPS cells with that from control iPS cells that were generated from healthy donors. SCN-iPS and control iPS cells were cocultured with a 15-Gy-irradiated murine stromal cell line (the AGM-S3 cell line), as reported (13). After 12 d, the cocultured cells were harvested, and the $CD34^+$ cells separated from these cells (SCN-iPS–$CD34^+$ and control iPS–$CD34^+$ cells, respectively) were cultured in a hematopoietic colony assay by using a cytokine mixture (*Materials and Methods*). The number and size of the erythroid (E) and mixed-lineage (Mix) colonies derived from SCN-iPS–$CD34^+$ cells (1×10^4 cells) were nearly identical to those of the corresponding colonies derived from control iPS–$CD34^+$ cells (E colonies: SCN-iPS cells, 11.0 ± 3.0, and control iPS cells, 11.4 ± 3.9; Mix colonies: SCN-iPS cells, 25.1 ± 7.2, and control iPS cells, 17.4 ± 4.0) (Fig. 1 *B* and *C* and Fig. S2 *A* and *B*). However, the number of myeloid colonies derived from SCN-iPS–$CD34^+$ vs. control iPS–$CD34^+$ cells was significantly lower (SCN-iPS cells, 47.4 ± 19.5; control iPS cells, 127.8 ± 17.9; $P < 0.01$), and the size of the colonies was also smaller (Fig. 1 *A*

Author contributions: T.H., Y.E., K.Y., S.M., S.Y., Y.F., K. Tani, H.N., M.K., and K. Tsuji designed research; T.H., Y.M., K.N., and K.Y. performed research; T.H., Y.E., Y.M., K.N., K.Y., K.U., N.N., S.M., S.Y., M.N., and K. Tsuji analyzed data; and T.H., Y.E., and K. Tsuji wrote the paper.

The authors declare no conflict of interest.

This article is a PNAS Direct Submission. G.Q.D. is a guest editor invited by the Editorial Board.

[1]To whom correspondence should be addressed. E-mail: ebihara@ims.u-tokyo.ac.jp.

This article contains supporting information online at www.pnas.org/lookup/suppl/doi:10.1073/pnas.1217039110/-/DCSupplemental.

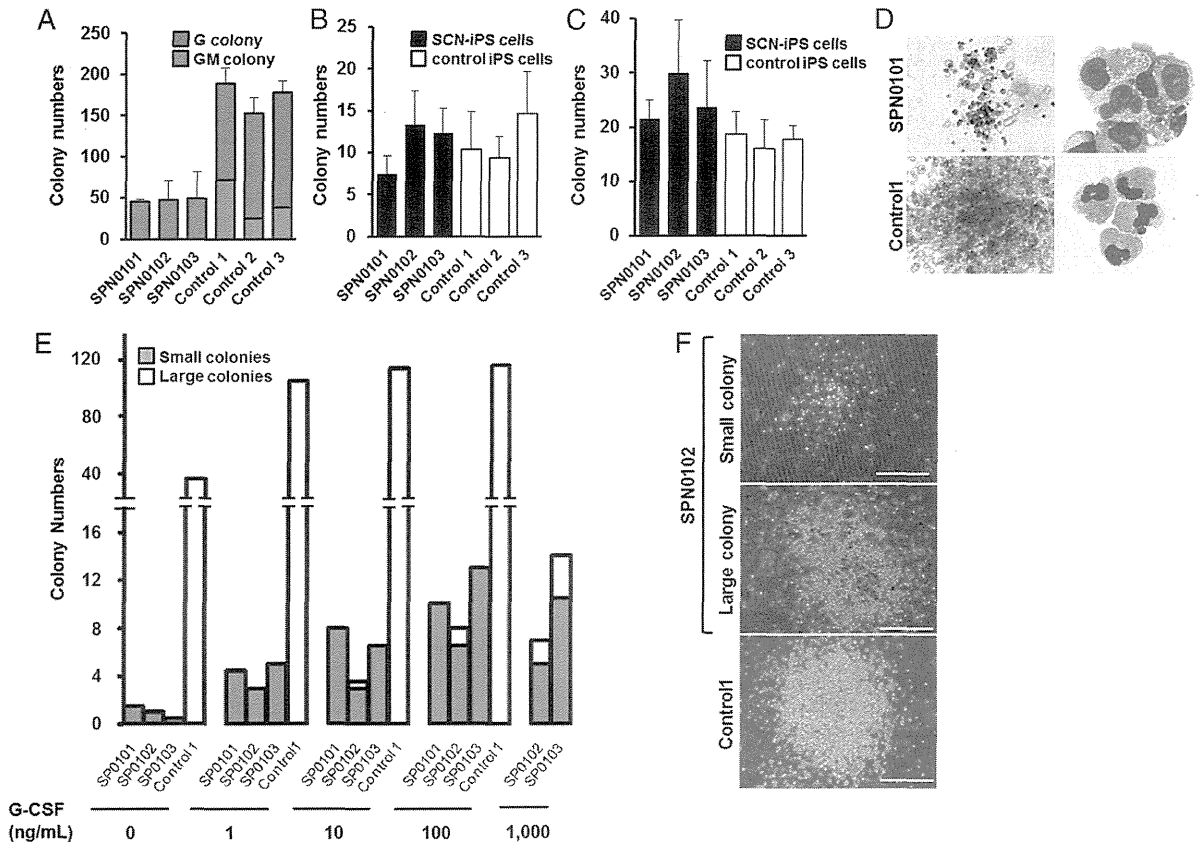

Fig. 1. Impaired neutrophil development from SCN-iPS cells. (*A–C*) A hematopoietic colony assay was performed by using 1×10^4 $CD34^+$ cells derived from three SCN-iPS cell clones (SPN0101, SPN0102, and SPN0103) and three control iPS cell clones (controls 1, 2, and 3) in the presence of a cytokine mixture. Colonies were sorted as myeloid (*A*), erythroid (*B*), and mixed-lineage (Mix) (*C*). Data are shown as mean ± SD. (*D*) Photographs of colonies (*Left*; 100×) and cells in a GM colony (*Right*; 400×; May–Grünwald–Giemsa staining). (*E*) A hematopoietic colony assay with dose escalation of G-CSF was performed by using 1×10^5 $CD34^+$ cells derived from SCN-iPS and control iPS cells. Filled and open bars indicate small colonies consisting of <100 cells and large colonies consisting of >100 cells, respectively. Data are shown as the average of three independent experiments. (*F*) Photographs of a small colony derived from SCN-iPS cells (SPN0102) in the presence of 10 ng/mL G-CSF, large colonies derived from SCN-iPS cells in the presence of 1,000 ng/mL G-CSF, and large colonies derived from control iPS cells (control 1) in the presence of 10 ng/mL G-CSF. (Scale bars, 200 μm.)

and *D*). In particular, only a few SCN-iPS cell-derived granulocyte (G) colonies—myeloid colonies consisting of only granulocytes—were detected (Fig. 1*A*). SCN-iPS cell-derived granulocyte–macrophage (GM) colonies—myeloid colonies consisting of macrophages/monocytes with/without granulocytes—contained a few immature myeloid cells in addition to macrophages/monocytes, whereas control iPS cell-derived GM colonies included a substantial number of mature, segmented, and band neutrophils (Fig. 1*D*).

We also found that Mix colonies derived from SCN-iPS cells, but not control iPS cells, contained immature myeloid cells and few mature neutrophils (Fig. S2 *C* and *D*). Next, we conducted a hematopoietic colony assay using various concentrations of G-CSF alone instead of the cytokine mixture to examine the G-CSF dose dependency of neutrophil differentiation from SCN-iPS and control iPS–$CD34^+$ cells. For all concentrations of G-CSF used (1–1,000 ng/mL), the SCN-iPS cell-derived myeloid colonies were significantly lower in number and smaller in size than the control iPS cell-derived myeloid colonies (Fig. 1*E*). Myeloid colony formation from control iPS cells reached a plateau at ~1–10 ng/mL G-CSF, whereas the number and size of those from SCN-iPS cells gradually increased with increasing concentrations of G-CSF. However, the values observed for SCN-iPS cells did not reach those for the control iPS cells, even at the highest dose of G-CSF used (1,000 ng/mL). Furthermore, large colonies consisting of >100 cells derived from SCN-iPS cells were only found with higher concentrations of G-CSF (Fig. 1*F*). Thus, granulopoiesis initiated from SCN-iPS cells was relatively insensitive to G-CSF, reflecting the inadequate in vivo response of neutrophils to G-CSF in SCN patients (14, 15). Therefore, these results support the applicability of the SCN-iPS cells established herein as a disease model for SCN.

To examine neutrophil development from SCN-iPS cells in more detail, SCN-iPS and control iPS–$CD34^+$ cells (1×10^4 cells each) were cocultured in suspension with AGM-S3 cells in the presence of neutrophil differentiation medium (*SI Materials and Methods*). The number of nonadherent cells derived from SCN-iPS–$CD34^+$ cells was lower than that from control iPS–$CD34^+$ cells on day 14 of culture (SCN-iPS cells, $9.77 \times 10^4 \pm 1.65 \times 10^4$ cells; control iPS cells, $52.48 \times 10^4 \pm 23.13 \times 10^4$ cells; $P < 0.05$) (Fig. 2*A*). The proportion of mature neutrophils among the nonadherent cells was also significantly lower for SCN-iPS cells relative to control iPS cells on day 14 (SPN-iPS cells, 15.53% ± 4.33%; control iPS cells, 71.285 ± 3.30%; $P < 0.05$) (Fig. 2 *B* and *C*), indicating that myeloid cells derived from SCN-iPS cells revealed the maturation arrest in the neutrophil development. We then examined a possibility that the maturation arrest in SCN-

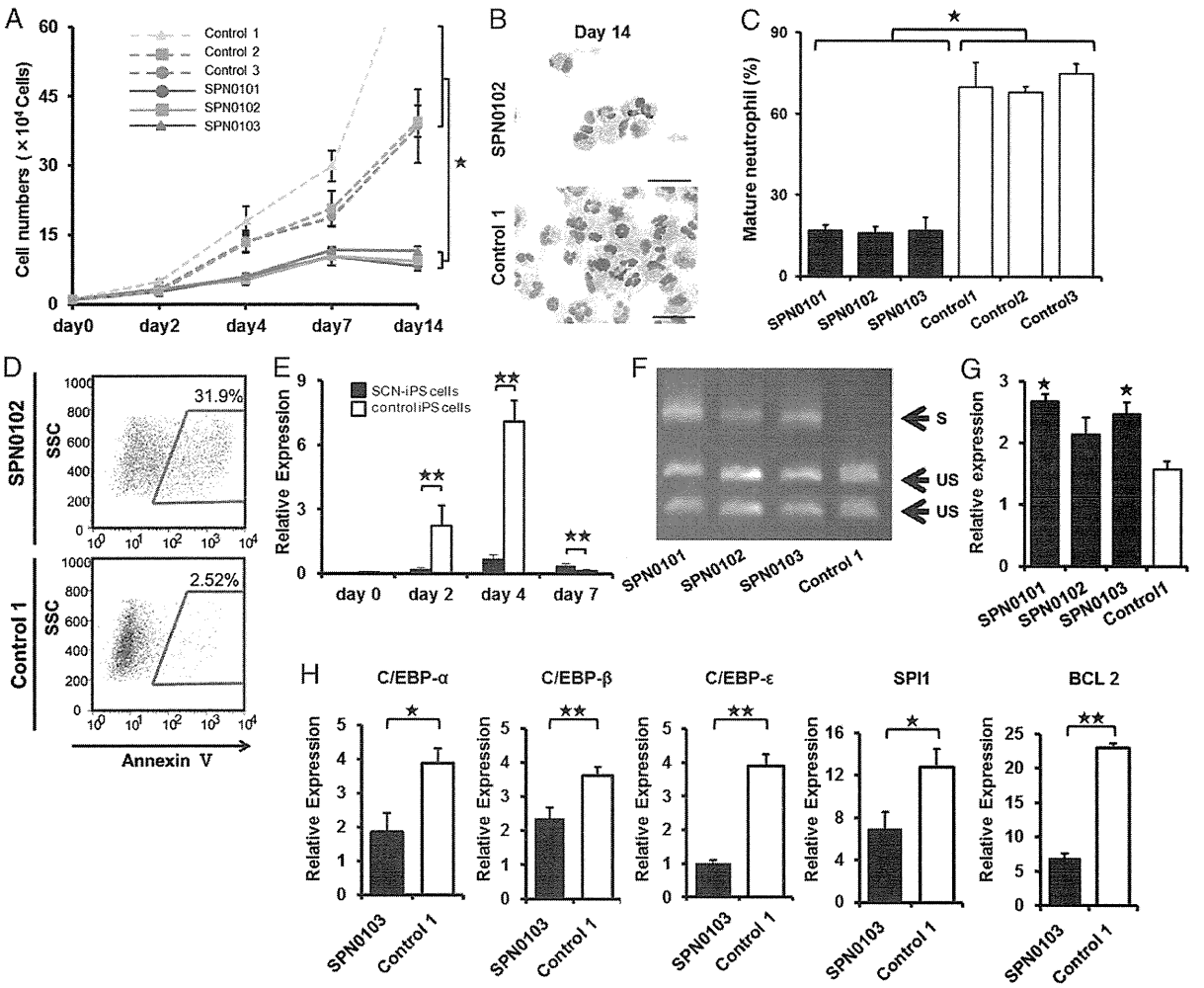

Fig. 2. Analysis of impaired neutrophil development from SCN-iPS cells. (*A*) Total number of nonadherent cells in the suspension culture of 1×10^4 $CD34^+$ cells derived from SCN-iPS and control iPS cells. Data are shown as mean ± SD. $^*P < 0.01$. (*B*) Photographs of nonadherent cells derived from SCN-iPS (SPN0103) and control iPS cells (control 1) on day 14 of culture (400×; May–Grünwald–Giemsa staining; scale bars, 50 μm.) (*C*) Filled and open bars show the proportion of mature neutrophils among the cells derived from SCN-iPS (filled bars) and control iPS (open bars) cells on day 14 of suspension culture. Data are shown as mean ± SD. $^*P < 0.05$. (*D*) Flow cytometric analysis of annexin V expression on cultured cells from SCN-iPS cells (SPN0102) or control iPS cells (control 1) on day 7. (*E*) Sequential qRT-PCR analysis of the relative expression of ELANE mRNA [ELANE/hypoxanthine–guanine phosphoribosyltransferase (HPRT) expression]. Data obtained from independent experiments using three SCN-iPS cell clones (SPN0101, SPN0102, and SPN0103) and three control iPS cell clones are shown as mean ± SD. $^{**}P < 0.01$. (*F* and *G*) $CD34^+$ cells derived from SCN-iPS or control iPS cells were cultured in neutrophil differentiation medium (see text). On day 7, nonadherent cells were collected and analyzed. (*F*) Representative gel showing spliced (S) and unspliced (US) XBP-1 bands on day 7. (*G*) qRT-PCR analysis of the relative mRNA expression (target/HPRT expression) of BiP on day 7. Data are shown as mean ± SD. $^*P < 0.05$; different from control 1). (*H*) qRT-PCR analysis of the relative mRNA expression (target / HPRT expression) of C/EBP-α, C/EBP-β, C/EBP-ε, SPI1, and BCL2 genes in non-adherent cells derived from SCN-iPS cells (filled bars, SPN0103) and control iPS cells (open bars, control 1) on day 2 of suspension culture. Data are shown as the mean ± the s.d. ($^{**}P < 0.01$, $^*P < 0.05$).

iPS cell-derived myeloid cells might be caused by their apoptosis. In flow cytometric analysis, SCN-iPS cell-derived myeloid cells contained a significantly higher proportion of annexin V-positive cells than control iPS-derived myeloid cells on day 7 of culture, suggesting that the maturation arrest in myeloid cells derived from SCN-iPS cells might be caused by their apoptosis (Fig. 2*D*).

We next examined ELANE mRNA expression levels in nonadherent cells derived from SCN-iPS vs. control iPS cells (Fig. 2*E*). ELANE expression was significantly lower in nonadherent cells derived from SCN-iPS vs. control iPS cells on days 2 and 4 of culture ($P < 0.01$), as reported (16, 17). However, the former was a little higher than the latter on day 7 ($P < 0.01$). This result may be explained by the existence of SCN-iPS cell-derived myeloid cells arrested at an early stage along the neutrophil differentiation pathway even on day 7 of culture. We also examined the expression of proteinase 3 and azurocidin, which comprise a family of closely related genes encoding neutrophil granule proteins along with ELANE, and found these genes were more highly expressed on day 4 (Fig. S3).

It has been reported that induction of the endoplasmic reticulum stress (ER) response and the unfolded protein response (UPR) has been advanced as a potential explanation for the molecular pathogenesis of SCN (18, 19). Thus, we examined activation of the UPR by X-box binding protein 1 (XBP-1) mRNA splicing on day 7. As shown in Fig. 2*F*, SPN-iPS cells induced XBP-1 mRNA splicing. We also found the up-regulation of BiP